

# Power-law friction in closely-packed granular materials

Takahiro Hatano

*Earthquake Research Institute, University of Tokyo, 1-1-1 Yayoi, Bunkyo, Tokyo 113-0032, Japan*

(Dated: February 21, 2019)

In order to understand the nature of friction in closely-packed granular materials, a discrete element simulation on granular layers subjected to isobaric plain shear is performed. It is found that the friction coefficient increases as the power of the shear rate, the exponent of which does not depend on the material constants. Using a nondimensional parameter that is known as the inertial number, the power-law can be cast in a generalized form so that the friction coefficients at different confining pressures collapse on the same curve. We show that the volume fraction also obeys a power-law.

Friction is one of the oldest problems in science because it dominates various phenomena in our daily life. In particular, flow dynamics of granular materials, which is ubiquitous in earth science and engineering, is governed by laws that describe behaviors of friction coefficient (ratio of shear stress to normal pressure). Such examples are avalanche, landslide, debris flow, silo flow, etc. In addition, the nature of friction on faults, which plays a key role in earthquake mechanics [1, 2], is also attributed to that of granular rock because fault zone consists of layers of fine rock granules that are ground-up by the fault motion of the past. To find suitable laws of friction in granular materials under specific conditions is thus an essential problem in natural science and engineering.

Although the frictional properties of granular materials are so important, our understanding is still limited. In the context of earthquake mechanics, sliding velocity (or shear rate) dependence of friction coefficient, which is equivalent to rheology under constant pressure condition, is a matter of focus because it determines dynamics of slip [2]. In experiments on thin granular layers subjected to relatively low sliding velocities ranging from nm/s to mm/s, the behavior of friction coefficient can be described by a phenomenological law in which friction coefficient logarithmically depends on slip velocity. This is known as the rate and state dependent friction (RSF) law [3]. Although the RSF law applies to low speed friction at interfaces between two solids as well as that in granular layers, it is not applicable to high speed friction. For example, several experiments indicated nonlogarithmic increase of friction coefficient in granular layers at higher slip velocities [4, 5, 6]. The same tendency was also observed in experiments on friction between two sheets of paper [7, 8]. Thus anomalous strengthening of friction at high velocities seems universal. However, at this point, we do not know any friction law that is valid at higher slip velocities.

In this paper, we perform a computer simulation on sheared granular layers under constant pressure in order to understand the nature of friction outside the region where the RSF law is valid. A new law is reported in which friction coefficient increases as the power of shear rate. This law describes friction in granular layers under

high shear rates and high pressure (on the order of tens of MPa) that may be relevant to seismic slip on faults.

Our computational model mimics a typical experiment on granular layers subjected to simple shear. The granules are assumed to be spherical particles, diameters of which range uniformly from  $0.7d$  to  $1.0d$ . The system spans  $L_x \times L_y \times L_z$  volume, and is periodic in the  $x$  and the  $y$  directions. In the  $z$  direction, there exist two parallel rough walls that consist of the same kind of particles as those in the bulk. The walls are displaced antiparallel along the  $y$  direction at a constant velocity  $V/2$  in order to cause plain shear flow whose velocity gradient is in the  $z$  direction. One of the walls is allowed to move along the  $z$  direction so that the pressure is kept constant at  $P$ , while the motion along the  $x$  direction is prohibited for both walls. Note that there is no gravity in the system.

The computational model is the discrete element method (DEM) [9]. Consider a grain  $i$  of radius  $R_i$  located at  $\mathbf{r}_i$  moving with the translational velocity  $\mathbf{v}_i$  and the angular velocity  $\boldsymbol{\Omega}_i$ . This grain interacts with another grain  $j$  whenever overlapped; i.e.  $|\mathbf{r}_{ij}| < R_i + R_j$ , where  $\mathbf{r}_{ij} = \mathbf{r}_i - \mathbf{r}_j$ . The interaction consists of two types of force, each of which is normal and transverse to  $\mathbf{r}_{ij}$ , respectively. Introducing the unit normal vector  $\mathbf{n}_{ij} = \mathbf{r}_{ij}/|\mathbf{r}_{ij}|$ , the normal force acting on  $i$ , which is denoted by  $\mathbf{F}_{ij}^{(n)}$ , is given by  $[f(\epsilon_{ij}) + \zeta \mathbf{n}_{ij} \cdot \dot{\mathbf{r}}_{ij}] \mathbf{n}_{ij}$ , where  $\epsilon_{ij} = 1 - |\mathbf{r}_{ij}|/(R_i + R_j)$ . A function  $f(\epsilon)$  describes elastic repulsion between grains. Here we test two models:  $f(\epsilon) = k\epsilon$  (linear force) and  $f(\epsilon) = k\epsilon^{3/2}$  (Hertzian force) [11]. Note that the constant  $k/d^2$  is on the order of the Young's modulus of the grains. In order to define transverse force, we utilize relative tangential velocity  $\mathbf{v}_{ij}^{(t)}$  defined by  $(\dot{\mathbf{r}}_{ij} - \mathbf{n}_{ij} \cdot \dot{\mathbf{r}}_{ij}) + (R_i \boldsymbol{\Omega}_i + R_j \boldsymbol{\Omega}_j)/(R_i + R_j) \times \mathbf{r}_{ij}$  and introduce relative tangential displacement vector  $\Delta_{ij}^{(t)} = \int dt \mathbf{v}_{ij}^{(t)}$ . Then tangential force acting on  $i$  is written as  $\min(\mu \dot{\mathbf{r}}_{ij}/|\dot{\mathbf{r}}_{ij}|, k_t \Delta_{ij}^{(t)}) |\mathbf{F}_{ij}^{(n)}|$ . In the case that  $\mu = 0$ , tangential force is absent so that the rotation of particles does not affect their dynamics.

We set  $d = 1$ ,  $m = 1$ ,  $k = 400$ , and  $k_t = k/2$ , where  $m$  and  $d$  denote the mass and the diameter of the largest particles, respectively. Note that the viscous coefficient  $\zeta$

together with  $k$  determines the coefficient of restitution. Here we investigate the case in which the coefficient of restitution almost vanishes ( $\zeta = 20$ ) unless otherwise indicated.

The system reaches a steady state after a certain amount of displacement of the walls. We confirm that the transient behaviors of the friction coefficient and of the volume increase are quite similar to those observed in experiments. Here we do not investigate such transients and restrict ourselves to steady-state friction.

Because uniform shear flow is unstable in a certain class of granular systems, we must check the internal velocity profiles at steady states. There is a strict tendency that shear flow is localized near the walls in the case that the confining pressure is high and/or the slip velocity is large. This kind of spatial inhomogeneity is rather ubiquitous in granular flow, and is extensively investigated by Nott et al. [10]. Note that uniform shear flow is realized at lower slip velocities and higher confining pressures in our simulation. In this paper, we discuss exclusively the case in which uniform shear is realized.

We investigate behaviors of the friction coefficient of the system, which is denoted by  $M$ . First we discuss the dependence of  $M$  on the shear rate,  $\gamma$ . Note that the shear rate is proportional to the slip velocity under uniform shear; i.e.,  $\gamma = V/L_z$ . In order to grasp the main point of our result, it is convenient to begin with the models in which friction between individual particles and rotation of particles are not incorporated. Recall that we test two models, each of which has different type of interaction. In the Hertzian force model, shear rate dependence of the friction coefficient is described by  $M \simeq (\gamma/\gamma_*)^\phi$  (see FIG. 1 a), where  $\phi = 0.26 \pm 0.02$  and  $\gamma_*$  is a constant that depends on the system parameters, such as the confining pressure and the stiffness of the particles. In the linear force model, the power-law is generalized to the following form.

$$M = M_0 + \left( \frac{\gamma}{\gamma_*} \right)^\phi, \quad (1)$$

where  $M_0$  denotes the friction coefficient for  $\gamma \rightarrow 0$ . We find that the rheology of the present model is described by Eq. (1) with  $\phi = 0.26 \pm 0.02$  in a wide range of the slip velocity. See FIG. 1 b.

In order to confirm universality of Eq. (1), we wish to show independence of our results on the details of the model. First we discuss effects of the tangential force between particles, which we do not consider in the above paragraph. As shown in FIG. 2, in the Hertzian force model, the friction coefficient obeys Eq. (1) with  $M_0$  being 0.27. Surprisingly, the exponent  $\phi$  is again approximately 0.26. This behavior is essentially the same as that of the linear force model. Indeed, in the case that  $\mu = 0.2$ , the friction coefficients of the Hertzian model and of the linear force model are almost the same. Note

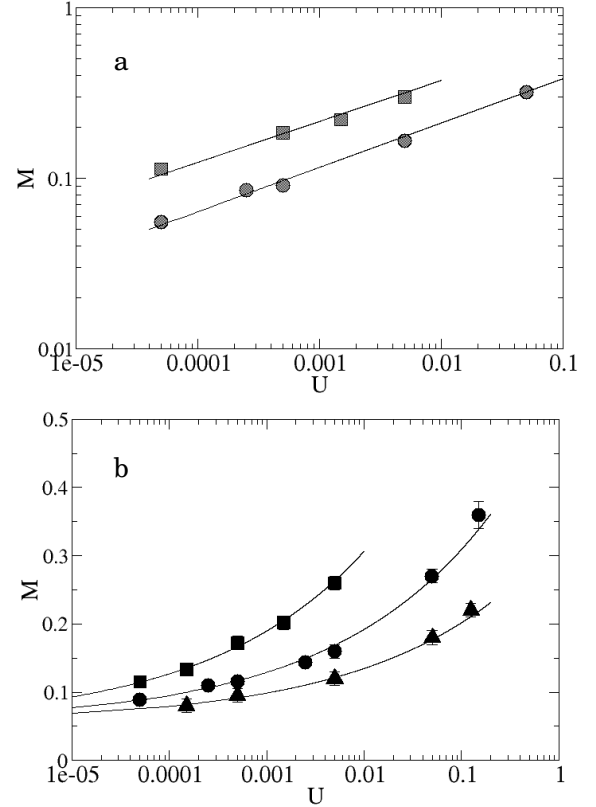


FIG. 1: Velocity dependence of the friction coefficient  $M$  in the model without tangential force, i.e.,  $\mu = 0$ . The horizontal axis  $U$  denotes the nondimensional velocity of the walls,  $V\sqrt{m/kd}$ . The shape of the symbols and the confining pressure are in one-to-one correspondence: circles to  $P/(k/d^2) = 0.76$ , squares to  $P/(k/d^2) = 0.015$ , and triangles to  $P/(k/d^2) = 1.57$ . The layer thickness is  $L_z/d \simeq 8$ , except for the triangles ( $L_z/d \simeq 26$ ). (a) Friction coefficient of the Hertzian force model. The lines are proportional to  $\gamma^\phi$ . (b) Friction coefficient of the linear force model. The lines denote Eq. (1).

that the friction coefficient of these models range from 0.3 to 0.4, which are not significantly discrepant from those obtained in an experiment on spherical glass beads [12].

Although the constant  $M_0$  in Eq. (1) looks like the static friction coefficient, note that  $M_0$  is defined in the  $\gamma \rightarrow 0$  limit and different from the static friction coefficient above which systems at rest begin to flow. In order to distinguish the two concepts,  $M_0$  is referred to as dynamic yield strength. The difference is important when we consider the stability of slip, as will be discussed in the last paragraph of this paper. The value of the dynamic yield strength depends on, but not equals to, the friction coefficient between individual grains,  $\mu$ . In the linear force model,  $M_0 \simeq 0.05$  for  $\mu = 0$ , while  $M_0 \simeq 0.26$  for  $\mu = 0.2$ , and  $M_0 \simeq 0.36$  for  $\mu = 0.6$ . Similar dependence was also observed in a two dimensional DEM simulation [13].

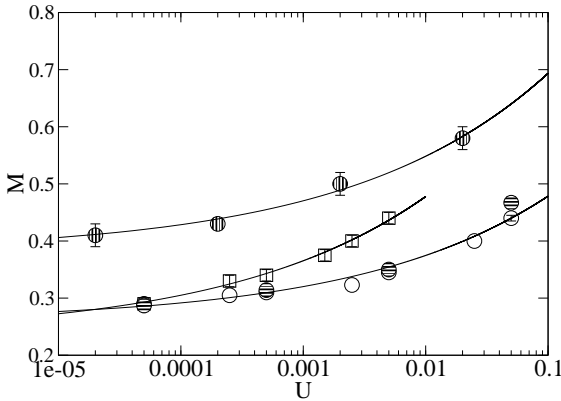


FIG. 2: Friction coefficients in the models with tangential force. The shape of the symbols and the confining pressure are in one-to-one correspondence: Circles to  $P/(k/d^2) = 0.76$  and squares to  $P/(k/d^2) = 0.015$ . The blank symbols denote friction coefficients of the linear force model in which  $\mu = 0.2$ , while the symbols of vertically-striped pattern denote those for  $\mu = 0.6$ . The circles of horizontally-striped pattern denote the Hertzian force model with  $\mu = 0.2$ . The lines denote Eq. (1).

Then we discuss the effects of the control parameters such as the confining pressure, the layer thickness, and the degree of inelasticity. First we discuss the effect of the confining pressure on the friction law, Eq. (1). Indeed, the pressure affects Eq. (1) only through the constant  $\gamma_*$ , and the exponent does not change. In order to see this more quantitatively, we use a nondimensional parameter known as the inertial number [14];  $I = \gamma\sqrt{m/Pd}$ . Then Eq. (1) can be cast in a generalized form in which the effect of the confining pressure is expressed through the inertial number  $I$ .

$$M = M_0 + s_1 I^\phi, \quad (2)$$

where  $s_1$  is a numerical factor. In FIG. 3, we can see that the friction coefficient at different pressures collapse on the same curve described by Eq. (2). Note that the layer thickness does not affect the friction law. However, inelasticity involving the normal interaction, which is modeled by the viscous coefficient  $\zeta$ , does affect frictional strength. We perform several runs of the simulation with different values of  $\zeta$ , and find that decrease of  $\zeta$  reduces the friction coefficient. This is quite reasonable because dissipation due to inelasticity leads to frictional resistance. Nevertheless, the friction coefficient is still described by Eq. (2) with  $s_1$  being a different value. But the functional form of  $s_1(\zeta)$  is not clear at this point.

From the discussions so far, we can conclude that the details of the present model do not affect the validity of Eq. (2), which is the main result of this paper. Importantly, the exponent  $\phi$  seems to be universal; it is approximately 0.26 regardless of the details of the model and the control parameters. The velocity-strengthening

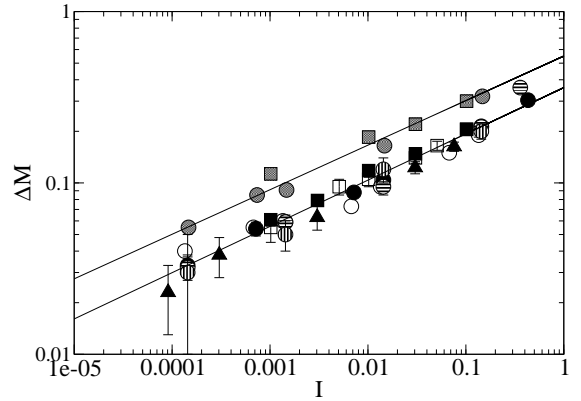


FIG. 3: The increase of the friction coefficient  $\Delta M = M - M_0$  is replotted as functions of the inertial number. The symbol legends are the same as those in FIGS. 1 and 2. The lines denote Eq. (2).

nature of this friction law does not contradict experiments [4, 5, 6, 7, 8]. In addition, it illustrates universality of power-law in rheological properties of random media [15, 16, 17], such as glassy materials [18, 19, 20], foams [21], and human neutrophils [22]. In the following we discuss four important points that are peripherally related to power-law friction.

First, we discuss the dependence of the volume fraction to the inertial number. Surprisingly, decrease of the volume fraction caused by shear flow is also described by a power-law.

$$\nu_0 - \nu = s_2 I^\delta, \quad (3)$$

where  $\nu_0$  is the volume fraction in the  $\gamma \rightarrow 0$  limit. Note that the constants  $s_2$  and  $\delta$  do not depend on the details of the model. Figure 4 shows that all of the data obtained in our model collapse on Eq. (3) with  $s_2 \simeq 0.11$  and  $\delta = 0.56 \pm 0.02$ . This dilatation law also illustrates the ubiquity of power-law in granular matter.

The next point we wish to discuss is the relation between the present result and power-law rheology in systems at constant volume. In particular, Xu and O'Hern [23] found a power-law relation between shear stress and shear rate in a two dimensional granular material consisting of frictionless particles. They estimated the exponent to be 0.65. However, at constant volume condition, pressure also depends on shear rate so that the behavior of friction coefficient is generally different from that of shear stress. Therefore, power-law rheology in systems under constant volume condition are not directly related to the present result. See Ref. [24]. for more detailed discussions on this subject.

The third point we wish to discuss is the effect of dimensionality. Da Cruz et al. simulated a two dimensional granular system that is sheared under constant pressure [13]. In contrast to the present study, they obtained a linear rheology expressed in terms of the inertial num-

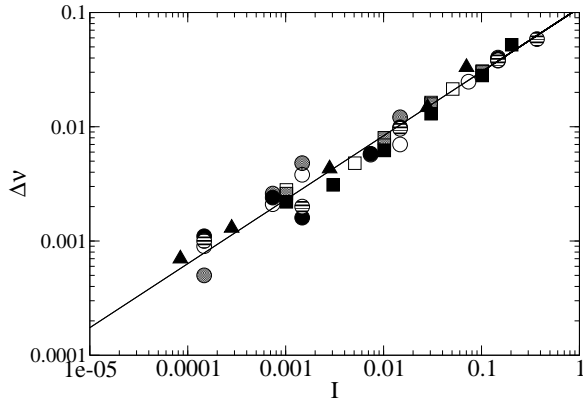


FIG. 4: The dilatation law. Decrease of the volume fraction  $\Delta\nu = \nu_0 - \nu$  is plotted as a function of the inertial number. Note that  $\nu_0$  is the volume fraction in the  $\gamma \rightarrow 0$  limit, which is estimated by extrapolation. The symbol legends are the same as those in FIG. 3. The line denotes Eq. (3).

ber; i.e.,  $\phi = 1$  in Eq. (2). The difference is attributed to the dimensionality of the systems, which affect the nature of contact between particles. In particular, the distribution of tangential force is strongly anisotropic in their two dimensional system, while such anisotropy is not observed in our three dimensional system. Accordingly, in the case that tangential force was switched off, their system exhibited a friction law that is quite similar to ours.

As the fourth point of interest, we discuss relevance of our result to earthquake mechanics by comparing it to a friction law recently proposed by Jop et al. [26], which seems to be validated in experiments on inclined plane flow. We stress that such flow is characterized by relatively large inertial number (typically  $10^{-1} \leq I \leq 10^0$ ), while our simulation involves much smaller values ( $10^{-5} \leq I$ ) as shown in FIG. 3. Such small inertial numbers correspond to configurations that are considered to be typical to seismic motion of faults. For example, in the case that  $d = 1$  mm,  $V = 1$  m/s,  $L_z = 4$  cm, and  $P = 100$  MPa, the corresponding inertial number is  $10^{-4}$ .

Because the friction law found here is velocity-strengthening, one may wonder that it cannot explain stick-slip motion. Recall that we discuss exclusively stationary-state dynamic friction. Taking static friction into account, unstable slip is inevitable because static friction is always stronger than dynamic friction, which is mainly due to dilatation [27]. Therefore power-law friction in stationary states does not contradict unstable slip on faults.

The author gratefully acknowledges helpful discussions with Hisao Hayakawa, Namiko Mitarai, Michio Otsuki, Shin-ichi Sasa, and Masao Nakatani.

---

- [1] K. Aki and P. G. Richards, *Quantitative Seismology* 2nd ed., (University Science Books, Mill Valley, 2002).
- [2] C. H. Scholz, *The mechanics of earthquakes and faulting*, (Cambridge University Press, Cambridge, 2002).
- [3] C. Marone, Ann. Rev. Earth Planet. Sci. **26**, 643 (1998).
- [4] M. L. Blanpied, T. E. Tullis, and J. D. Weeks, Geophys. Res. Lett. **14**, 554 (1987).
- [5] B. D. Kilgore, M. L. Blanpied, and J. H. Dieterich, Geophys. Res. Lett. **20**, 903 (1993).
- [6] M. L. Blanpied, T. E. Tullis, and J. D. Weeks, J. Geophys. Res. **103**, 489 (1997).
- [7] T. Baumberger, F. Heslot, and B. Perrin, Nature **367**, 544 (1994).
- [8] F. Heslot, T. Baumberger, B. Perrin, B. Caroli, and C. Caroli, Phys. Rev. E **49**, 4973 (1994).
- [9] P. A. Cundall and O. D. L. Strack, Geotechnique **29**, 47 (1979).
- [10] P. R. Nott, M. Alam, K. Agrawal, R. Jackson, and S. Sundaresan, J. Fluid Mech. **397**, 203 (1999).
- [11] K. L. Johnson, *Contact mechanics*, (Cambridge University Press, Cambridge, 1987).
- [12] J. L. Anthony, and C. Marone, J. Geophys. Res. **110**, B08409 (2005).
- [13] F. da Cruz, S. Emam, M. Prochnow, J.-N. Roux, and F. Chevoir, Phys. Rev. E **72**, 021309 (2005).
- [14] C. Ancey, P. Coussot, and P. Evesque, J. Rheol. **43**, 1673 (1999).
- [15] P. Sollich, Phys. Rev. E **58**, 738 (1998).
- [16] M. L. Falk and J. S. Langer, Phys. Rev. E **57**, 7192 (1998).
- [17] M. Otsuki and S. Sasa, cond-mat/0511111 (2005).
- [18] R. Yamamoto and A. Onuki, Europhys. Lett. **40**, 61 (1997).
- [19] F. Varnik, L. Bocquet, and J.-L. Barrat, J. Chem. Phys. **120**, 2788 (2004).
- [20] J. Rottler and M. O. Robbins, Phys. Rev. E **68**, 011507 (2003).
- [21] A. D. Gopal and D. J. Durian, Phys. Rev. Lett. **91**, 188303 (2003).
- [22] M. A. Tsai, R. S. Frank, and R. E. Waugh, Biophys. J. **65**, 2078 (1993).
- [23] N. Xu and C. S. O'Hern, Phys. Rev. E **73**, 061303 (2006).
- [24] T. Hatano, M. Otsuki, and S. Sasa, arXiv:cond-mat/0607511 (2006).
- [25] M. Nakatani, J. Geophys. Res. **106**, 13347 (2001).
- [26] P. Jop, Y. Forterre, and O. Pouliquen, Nature **441**, 727 (2006).
- [27] M. Nakatani, J. Geophys. Res. **103**, 27239 (1998).